

Figure 1: Updated merger fractions since last week (added three points).

1 Double Averaging

Last week, we mentioned wanting to verify that double averaging still holds at e_{lim} in the regime I am studying. Just to verify, I have computed a few quantities of interest for my fiducial parameter regime $a_{\text{in}} = 100 \text{ AU}$, $a_{\text{out,eff}} = 3600 \text{ AU}$:

$$\eta = 0.098 \left(\frac{q/(1+q)^2}{1/4} \right) (1 - e_{\text{out}}^2)^{1/4} \left(\frac{a_{\text{in}}}{100 \text{ AU}} \right)^{1/2} \left(\frac{3600 \text{ AU}}{a_{\text{out,eff}}} \right)^{1/2}, \quad (1)$$

$$t_{\text{LK}} = 3.42 \times 10^7 \text{ yr}, \quad (2)$$

$$P_{\text{in}} = 22 \text{ yr}, \quad (3)$$

$$P_{\text{out}} = 5300 \text{ yr}, \quad (4)$$

$$1 - e_{\text{max,DA}} = 1 - \sqrt{1 - \left(\frac{P_{\text{out}}}{t_{\text{LK}}} \right)^2} \approx 1.23 \times 10^{-6}. \quad (5)$$

Note that, for the fiducial parameter regime, $e_{\text{lim}} \approx 5 \times 10^{-7}$, but $e_{\text{os}} \approx 2 \times 10^{-6}$. Thus, while our GW-free simulations violate the DA criterion, the with-GW simulations are likely perfectly fine.

In fact, if we compare the expressions for e_{os} and $e_{\text{max,DA}}$ (or, more simply, $j = \sqrt{1 - e^2}$ for each), we find:

$$j_{\text{os}} \sim \left(\frac{t_{\text{LK}}}{t_{\text{GW},0}} \right)^{1/6}, \quad (6)$$

$$j_{\text{min,DA}} \sim \frac{P_{\text{out}}}{t_{\text{LK}}}. \quad (7)$$

Thus, DA is okay when $j_{\text{os}} \gtrsim j_{\text{min,DA}}$ (i.e. the binary will merge before DA breaks down). Maybe it's worth expressing this more carefully?

2 Effect on Observed Distribution of q

We start with a uniform distribution in $q \in [0.2, 1.0]$, and then we weight each q by its merger fraction in Fig. 1 to get the observed distribution over q . In other words,

$$P_{\text{merge}}(q) = \frac{P_{\text{primordial}}(q)f(e_{\text{out}}, q)}{\int_0^1 P_{\text{primordial}}(q)f(e_{\text{out}}, q) dq}, \quad (8)$$

where $f(e_{\text{out}}, q)$ is the merger probability in Fig. 1. The resulting plot is shown in Fig. 2.

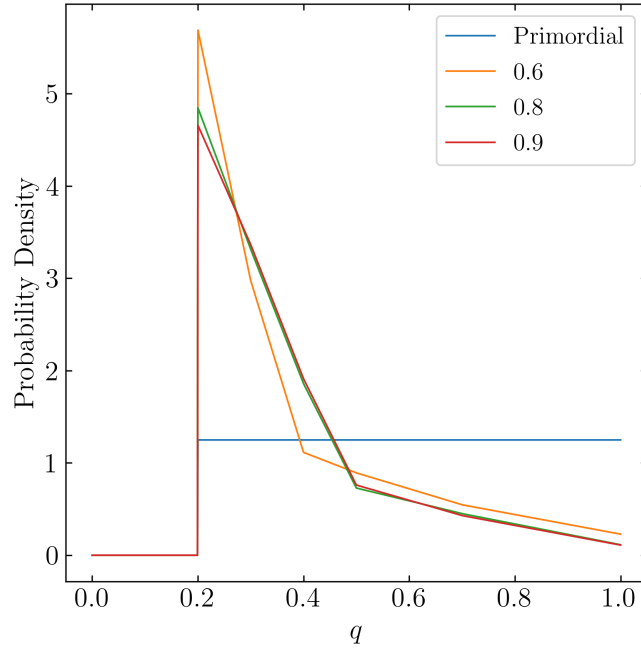


Figure 2: Normalized probability density functions for different e_{out} and q among binaries that merge.

3 Trying to Understand the e_{max} Curve

This is a tentative section. I saw that the e_{max} curve had a lot of structure, even in the broad band sections (a clear maximum eccentricity during the sections where $e_{\text{max}} < e_{\text{lim}}$). I thought that maybe there could be a conserved quantity analysis that yields this bound analytically. My first idea is very simple, but it doesn't produce the right results for nonzero η yet.

3.1 Test Mass Experiment

I describe it below, where I disregard SRFs for now:

- Consider the Hamiltonian

$$H(e_1, I_1, \omega_1, e_2, I_2, \omega_2) = H_{\text{quad}}(e_1, I_1, \omega_1, e_2, I_2) + \epsilon_{\text{oct}} H_{\text{oct}}(e_1, I_1, \omega_1, e_2, I_2, \omega_2). \quad (9)$$

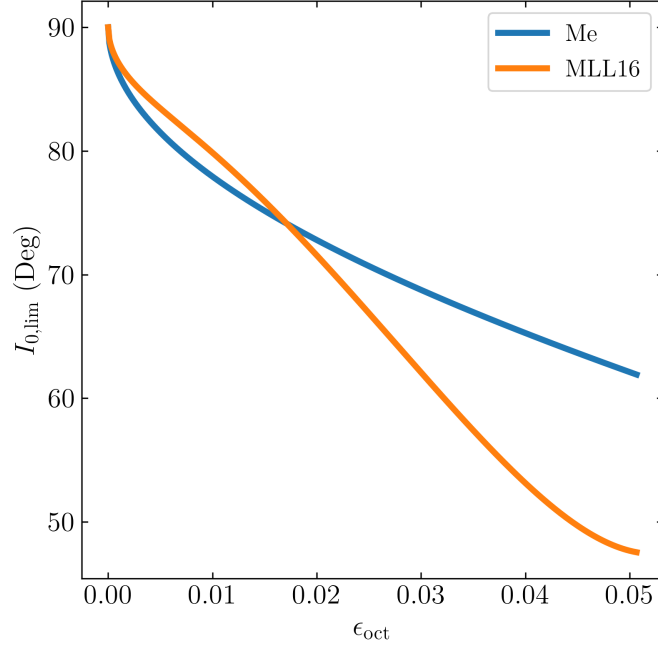


Figure 3: I_{lim} window for test particle case, using criterion Eq. (11), compared to MLL fitting formula. While inaccurate, the qualitative behavior is mildly encouraging.

Analytical forms for these exist in Naoz et al. 2011. By using the law of sines and conservation of total angular momentum, we can invert to find $e_2(e_1, I_1)$ and $I_2(e_1, I_1)$ as a function of $\eta_0 = L_{\text{in},0}/L_{\text{out},0}$. Thus, the Hamiltonian can be re-expressed implicitly

$$H(e_1, I_1, \omega_1, \omega_2) = H_{\text{quad}}(e_1, I_1, \omega_1) + \epsilon_{\text{oct}} H_{\text{oct}}(e_1, I_1, \omega_1, \omega_2). \quad (10)$$

- H is conserved. Examining the expressions in Naoz et al. 2011 (I think they have an extra factor of e_2 in their octupole potential? I may have misread, I haven't been very careful), it is clear that $H_{\text{oct}}/\epsilon_{\text{oct}}$ is bounded. Let's first assume that, over time, H_{oct} explores all available values.

Under this assumption, we can quantify whether an initial H_{quad} is “sufficiently close” to $H_{\text{quad},\text{lim}}$ (which, for simplicity, we take $H_{\text{quad},\text{lim}} = H_{\text{quad}}(0, 90^\circ, 0)$). In other words, one seemingly necessary condition for being in the octupole-active window is

$$H_{\text{quad},0} - H_{\text{quad},\text{lim}} \leq H_{\text{oct},\text{max}} - H_{\text{oct},0}, \quad (11)$$

where $H_{\text{oct},\text{max}}$ is taken over all values of $(e_1, I_1, \omega_1, \omega_2)$ for simplicity (this is obviously not quite correct). For each ϵ_{oct} , the I_0 (mutual inclinations) for which this condition is satisfied is shown in Fig. 3.

At first glance, this suggests that there is a chance we can bound the octupole-induced e_{max} oscillations. There are a few caveats:

- We maximized H_{oct} for all e_1, I_1 , which includes unreasonable values like $e_1 = 1, I_1 \approx 90^\circ$. When ϵ_{oct} is not too large, each individual LK cycle retains its shape, which suggests that

the maximum attainable H_{oct} is somewhere around $I_1 \approx 90^\circ$, $e_1 = e_{\min} \lesssim 0.5$. This can be confirmed with our old plots.

- When my window is too wide, a simple explanation exists: H_{oct} doesn't fully explore its parameter regime (also, the above effect means I overpredict the actual accessible $H_{\text{oct,max}}$).
- When instead my window is too small, this is possibly because the actual e_{lim} window is slightly larger than $I = 90^\circ$. In my model, $e_{\text{lim}} = 1$. Generalizing to $e_{\text{lim}} < 1$ is not hard, we just have to add a constant offset to $H_{\text{quad,lim}}$ in Eq. (11).

3.2 Failure with Finite Mass

However, this clearly fails to produce certain features of the $\eta > 0$ regime:

- H is symmetric about $I = 90^\circ$, the mutual inclination. We know that the actual e_{max} curve is maximized at $I_{\text{lim}} > 90^\circ$.
- H is quadratic in I , so it has only one minimum. This means that the criterion Eq. (11) must predict a single octupole-active zone, near the minimum. We observe a gap.

I would like some more ideas if possible! One I noticed is that the Katz, Dong, & Malhotra result has equations like

$$\frac{d(j \cos I)}{dt} \propto \epsilon_{\text{oct}} \sin \theta, \quad \frac{d\theta}{dt} \propto (j \cos I). \quad (12)$$

This implies that, if $I \approx 90^\circ$, the quadrupole-conserved quantity (in the test mass case) executes small oscillations near 90° .

3.3 Numerical Exploration of Octupole-induced K Oscillations (New)

Motivated by the above observation, we consider the range of oscillations in the quadrupole-conserved quantity for nonzero η :

$$K \equiv j \cos I - \eta_0 \frac{e^2}{2j_{\text{out}}}. \quad (13)$$

We have expressed in terms of η_0 because j_{out} can vary with octupole terms. We perform a similar analysis to the above: to quadrupolar order, K is constant, but including octupole effects, K oscillates. By attempting to bound the range of oscillation, we can understand which regions can reach

$$K_{\text{crit}} \equiv K(e = 0, I = I_{\text{lim}}). \quad (14)$$

It is suspected that for I sufficiently near 90° , the range of oscillation goes to zero, and K cannot reach K_{crit} . This is indeed the picture borne out by numerical simulations, as seen in Fig. 4.

It is clear that there is a lot of structure to this K plot, and that indeed there should be some sort of analytical bound the range of oscillation in K . However, unlike the analysis for H , it is not evident how the octupole-induced oscillations in K can be bound.

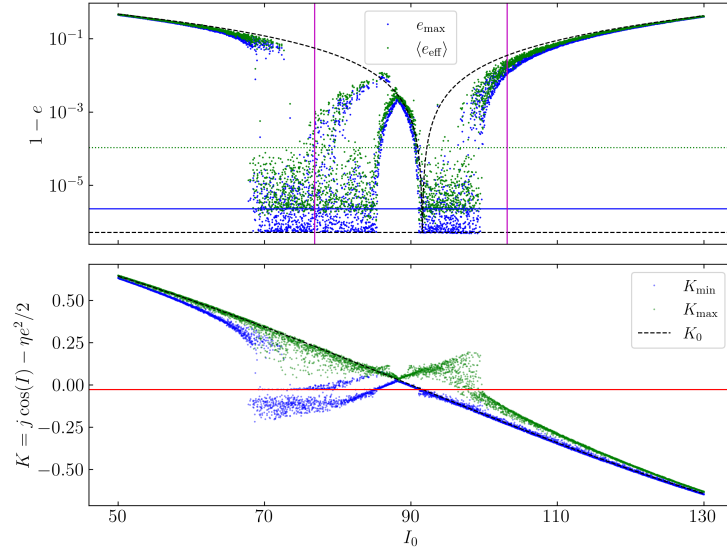


Figure 4: Plot of e_{\max} (top panel) and the range of oscillation of K (evaluated at eccentricity maxima) for $q = 0.2$ and $e_{\text{out},0} = 0.6$. Each I_0 is run 5 times. The black dashed line is K evaluated for initial conditions, and the horizontal red line is K_{crit} . It is clear that the origin of the gap is due to the limited oscillation in K .